Stability of Dendritic Crystals

David A. Kessler
Department of Physics, University of Michigan, Ann Arbor, Michigan 48109

and

Herbert Levine
Schlumberger-Doll Research, Ridgefield, Connecticut 06877
(Received 11 August 1986)

We present an integrodifferential-operator formulation of the problem of linear stability around the selected needle crystal pattern in dendritic crystal growth. We show by explicit computation that (a) all members of the discrete set of allowed steady states aside from the fastest are *unstable* and (b) the fastest such shape is linearly stable at least for large enough anisotropy. We comment on the implications of our work for the issue of side-branch wavelength determination.

PACS numbers: 61.50.Cj

Over the past several years, remarkable progress has been made in the field of interfacial pattern formation. One important example of this progress is the resolution of the long-standing problem of velocity selection for free-space dendritic crystals.[1] Specifically, it has been shown both numerically[2] and analytically[1,3] that inclusion of finite surface tension leads to a nontrivial solvability condition which selects a discrete set of possible steady-state shapes from the Ivantsov continuous family. This mechanism, usually referred to as "microscopic solvability," also explains pattern selection in other systems including the Saffman-Taylor finger[4] and directional solidification.[5]

The purpose of this paper is to provide the next stage in the study of dendritic crystal growth, an analysis of linear stability. Stability analysis (linear and finite amplitude) should ultimately resolve two issues. First, we need an explanation for the fact that although all members of the discrete set are allowed by the solvability condition, experiments consistently find only one unique pattern. Secondly, needle crystals are only found in nature in extremely anisotropic systems. Most often, the needle crystals break down via an instability to a full dendritic pattern, replete with side branches of fixed wavelength. The stability analysis should predict this wavelength as well as the boundary in parameter space between dendrites and needle crystals.

There have been some previous attempts at the study of dendritic stability. The classic papers of Langer and Müller-Krumbhaar[6] studied stability around the zero-anisotropy Ivantsov parabola (plus possibly a *perturbative* shape correction) for small Peclet number. This work was hampered by the fact that the "correct" Ivantsov parabola was unknown and, therefore, no predictions could be made regarding stability of the actual needle crystal. A more recent attempt by Pelce[7] resorted to the somewhat *ad hoc* WKB approximation introduced originally by Zeldovich *et al.*[8] This method, which predicts linear stability, is not sufficiently powerful to detect discrete mode instabilities and cannot distinguish among different members of the allowed discrete set. Our method, which relies on the *exact* numerical solution of the steady-state equation followed by numerical diagonalization of a resulting linear operator, is much more powerful, applicable at all Peclet numbers, and generalizable to all other interfacial pattern-forming systems. A discussion of the stability of the Saffman-Taylor finger with use of this method will appear elsewhere.[9]

The evolution equation for two-dimensional free-space dendrites growing under thermal diffusion limited conditions is well known:

$$\Delta - d_0(\theta)\kappa = \int ds'dt' G(\mathbf{x}(s)-\mathbf{x}(s');t-t')v_n(x',t'), \tag{1}$$

where Δ is the dimensionless undercooling $[(T_M - T_\infty)/(L/c_p)$ for latent heat L, specific heat c_p, melting temperature $T_M]$, κ is the two-dimensional curvature, v_n is the normal velocity of the interface $\mathbf{x}(s)$, and G is the two-dimensional diffusion kernel. The length $d_0(\theta)$, referred to as the capillary length, is taken to be

$$d_0(\theta) = \frac{c_p \gamma_0 T_M}{L^2}(1-\varepsilon\cos 4\theta) \equiv \bar{d}_0(1-\varepsilon\cos 4\theta), \tag{2}$$

where γ_0 is the surface tension and ε is the coefficient of fourfold crystal anisotropy depending on the angle θ between the interface normal $\hat{\mathbf{n}}$ and crystal axes.

If we assume that $\mathbf{x}(s) = \mathbf{x}_0(s) + v\hat{\mathbf{y}}t + \hat{\mathbf{n}}\delta$ for small δ, we arrive at the steady-state equation

$$\Delta - \gamma(\theta)\kappa = \int dx' K_0(R) e^{-(y-y')}, \tag{3}$$

with $\gamma = vd_0/2D$, $R = [(x-x')^2 + (y-y^1)^2]^{1/2}$, and K_0 the Bessel function (modified Hankel function); and the

linear stability equation

$$-\gamma(\theta_0)\kappa^{(1)}[\delta]-\kappa_0\gamma^{(1)}[\delta]=\int ds'\{\delta(s)\hat{\mathbf{n}}\cdot\nabla-\delta(s')\hat{\mathbf{n}}'\cdot\nabla'+v^{(1)}[\delta(s')]\}[K_0(R)e^{-(y-y')}], \tag{4}$$

where $\kappa^{(1)}[\delta]=-\delta''-\kappa_0^2\delta$ for initial curvature $\kappa_0(s)$,

$v^{(1)}[\delta]=\dot{\delta}-\hat{\mathbf{t}}_0\cdot\hat{\mathbf{y}}\delta'+\kappa_0\delta$, $\gamma^{(1)}[\delta]=\bar{\gamma}(+4\varepsilon\sin 4\theta_0\delta')$, and $\hat{\mathbf{t}}_0$ is the tangent vector of the initial interface. In Eq. (3), $\bar{\gamma}=v\bar{d}_0/2D$ is to be found as part of the solution. Note that in deriving the above stability equation, we have used the standard quasistatic approximation and neglected the time dependence of δ in all terms other than the velocity.

The first stage in our computation is to solve Eq. (3) for the allowed steady-state shapes. The procedure for doing this was first established by Vanden-Broeck[10] and extended to this system by us and independently by Meiron.[2] The basic finding of these papers is that no solutions exist for isotropic surface tension ($\varepsilon=0$) and that a discrete, possibly infinite set of different allowed values of $\bar{\gamma}$ exists at $\varepsilon\neq 0$. This discrete set is labeled by $\{\gamma_i\}$, the *largest* of which is $\bar{\gamma}_1$. Later, analytic methods led to the prediction that all solutions should obey the scaling $\gamma_i\sim\varepsilon^{7/4}$, a result in at least qualitative agreement with the numerical data at all values of the undercooling.

Once a particular steady-state solution $\bar{\gamma}_i, y_i(x)$ is known, we can proceed to evaluate numerically the linear stability operation. We discretize the curve by writing

$$u_j=\frac{ju_{\max}}{N_{\text{pts}}},\quad 1+\frac{2x_j^2}{N_{\text{Pe}}^2}=\left(1+\frac{4u_j^2}{N_{\text{Pe}}^2}\right)^{1/2},$$

where N_{pts} is the number of points, and similarly define y_j as $y(x_j)$ and δ_j as $\delta(s(x_j))$. Note that for small x, $x\sim u$ whereas for large x, $x^2\sim u$. The Peclet number $N_{\text{Pe}}=\rho_0 v/2D$ is found by determination of the tip radius ρ_0 of the Ivanstov parabola at undercooling Δ; $\Delta=(\pi N_{\text{Pe}})^{1/2}\exp(N_{\text{Pe}})\operatorname{erfc}(N_{\text{Pe}}^{1/2})$. The perturbation is required to vanish at distances past $u_{\max}$. The results must be then extrapolated to infinite cutoff $u_{\max}$ and discretization $u_{\max}/N_{\text{pts}}$ to derive the physical spectrum.

We schematically rewrite Eq. (4) as

$$A_{ij}^{[0]}v_{jk}^{(1)}\delta_k=A_{ij}^{[1]}\delta_j,$$

where ω is the eigenvalue and $v^{(1)}$, $A^{[0]}$, and $A^{[1]}$ are $N_{\text{pts}}\times N_{\text{pts}}$ matrices. The explicit expression for $A^{[1]}$ is derived by use of standard three-point discretization for all derivatives and replacement of the integral over s' by the trapezoidal rule. This procedure is accurate to $O(N_{\text{pts}}^{-2})$. $A^{[0]}$ is slightly more complicated because the logarithmic singularity in the Bessel functions prevents a simple discretization. We therefore replace the expression

$$\int ds' v^{(1)}[\delta(s')]K_0(R)e^{y'-y}$$

by

$$\int ds'\{v^{(1)}[\delta(s')]-v^{(1)}[\delta(s)]\}K_0(R)e^{y'-y}+v^{(1)}[\delta(s)]\int K_0(R)e^{y'-y}.$$

The first term has no singularity and the second equals $v^{(1)}[\delta(s)][\Delta-\gamma(\theta)\kappa_0]$ via the steady-state equation. We then invert $A^{[0]}$ numerically and define the linear operator $L\delta=(A^{[0]})^{-1}A^{[1]}\delta+\hat{\mathbf{t}}_y\delta'-\kappa_0\delta$. Finally, we truncate to an $M_{\text{pts}}\times M_{\text{pts}}$ submatrix of L, where M_{pts} is some number $<N_{\text{pts}}$, in order to minimize boundary effects; in practice, $M_{\text{pts}}\sim\frac{1}{2}N_{\text{pts}}$ is sufficient. This submatrix is diagonalized by use of an EISPACK QR algorithm.[11] For simplicity, we have only studied the case of symmetric modes and hence the index i only ranges over positive values. In the presence of crystal anisotropy, symmetric modes (tip splitting and/or side branching) are expected to be of much greater significance than antisymmetric modes, but this needs to be verified.

One stringent test on the validity of this approach and the correctness of the code is the existence of a translation zero mode. At all allowed solutions, there must be one mode at $\omega=0$. As a test, we generated a 150-point solution of the steady-state equation at $N_{\text{Pe}}=0.25$, $\varepsilon=0.25$; this solution has $\bar{\gamma}=2.899\times10^{-3}$. We then generated $y(x)$ via a spline routine, determined y_j and x_j accordingly, and ran the stability program at (M_{pts}, N_{pts}, $u_{\max}$) of (100, 200, 7.5) and (150, 300, 7.5). (One useful way of thinking about the discretization scale is to recognize that for these typical values of our numerical cutoffs, it varies from 0.01 to 0.1 of the tip size.) The translation mode could be extrapolated to occur at $\omega\sim1\times10^{-3}$, a factor of 5000 smaller than any other mode (see later). This value is consistent with our estimates of steady-state solution error and can be systematically improved by going to more points. It is insensitive to $u_{\max}$ once it is large enough (≥ 6).

At all values of ε which we have studied, the spectrum consists of three distinct pieces. At large negative Reω there is a real continuum with Im$\omega=0$. The end of the real continuum occurs at a point on the negative Reω axis. From there, a complex continuum emerges and continues to a maximum growth rate which is still negative. This part of the spectrum is plotted in Fig. 1 for the $\varepsilon=0.25$ case discussed above, at (250, 500, 10.0). Variation of $u_{\max}$ changes the spectrum slightly. However, just as was the case in a previous study[12] of the Saffman-Taylor finger, no continuum mode is *unstable*.

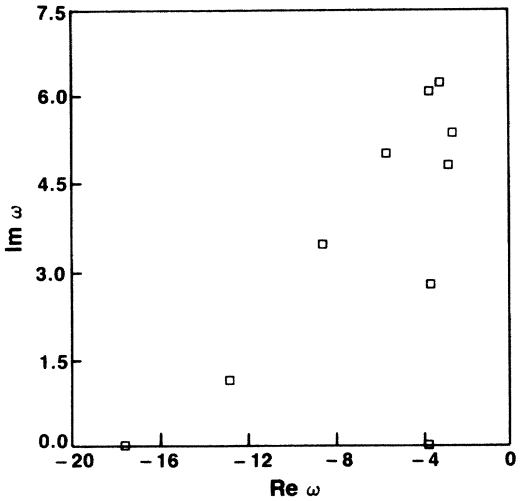

FIG. 1. Complex continuum at $\varepsilon=0.25$, and $\gamma=2.899\times10^{-3}$.

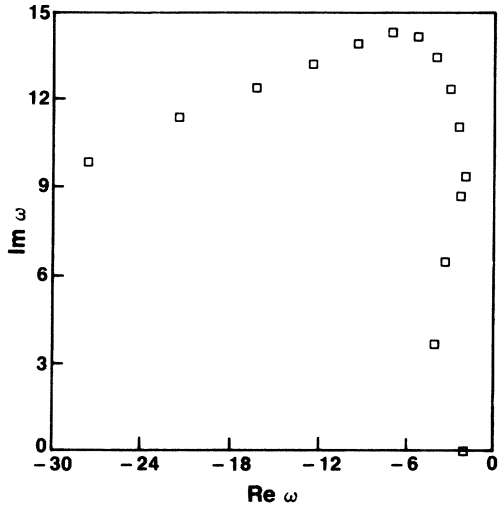

FIG. 2. Complex continuum at $\varepsilon=0.75$, $\gamma=6.56\times10^{-4}$.

This result is true at all values of the cutoff parameters. We have verified the absence of continuum-mode instabilities for all $\varepsilon\geq0.075$ at $N_{Pe}=0.25$. We have checked that this type of behavior for the continuous spectrum is qualitatively independent of N_{Pe}. Later, we comment on what might be expected at very low ε and how this issue relates to the determination of side-branch spacing. We now turn to the major result of this work, a computation of the discrete mode instabilities.

At $\varepsilon=0.25$, the case considered so far corresponds to the largest velocity pattern. Here, there is one additional discrete mode at $\omega=-3.6$. Hence, this steady-state solution is linearly stable. Next, we computed the second allowed solution at $\varepsilon=0.25$, which occurs at $\bar{\gamma}_0=2.96\times10^{-4}$. Now, there are discrete modes at $\omega=+12.5$, 0, and -2.3. Therefore, there is a discrete-mode instability which prevents this particular steady-state pattern from ever being observed experimentally. The eigenmode corresponding to the positive ω eigenvalue decays away from the tip, and hence can be interpreted as a tip-region instability.

We have done a similar study at $N_{Pe}=0.25$, $\varepsilon=0.4$. Now, the fastest *three* solutions correspond to $\bar{\gamma}_1=4.721\times10^{-3}$, $\bar{\gamma}_2=5.16\times10^{-4}$, $\bar{\gamma}_3=1.65\times10^{-4}$. All of these solutions give rise to stability operators for which the translation mode is $\sim10^{-3}$–10^{-1}, which is a measure of the accuracy of our numerics. The corresponding discrete mode spectra at these three values are respectively $\{0,-6.6\}$, $\{+11.34,0,-2.92\}$, and $\{+26.6, +15.03,0,-0.9\}$. Note that the third solution now has two unstable modes! The sum total of all our runs at differing parameter values provides incontrovertible evidence for the following scenario: As $\bar{\gamma}$ is lowered at fixed ε and N_{Pe}, we pass through a discrete set of allowed values corresponding to steady-state solutions of the interfacial evolution equation. Each additional solution has one additional tip-splitting instability. As we approach $\gamma=0$, we approach the completely unstable spectrum of tip-splitting modes expected for the Ivantsov parabola in the zero-surface-tension limit.

This type of spectral flow seems to be a necessary side effect of the solvability mechanism which gives rise to the discrete set of solutions. Prior to this work, it had been shown (first approximately,[12] later exactly[9]) that exactly the same scenario is valid for the Saffman-Taylor finger. We suspect that the WKB methods[1,3] that have recently been used to demonstrate the selection mechanism analytically can be extended to prove this property of the linear stability operator. This result means, of course, that finite surface-tension effects select a *unique* steady-state pattern for the physical system, a fact in agreement with generations of crystal growth experiments.

We have not yet seen any evidence for a *linear* instability or a marginal mode. Our calculations have extended all the way down to $\varepsilon=0.02$ and over the range $0.01<N_{Pe}<1$. For example, a graph at a 7.5% anisotropy, presented in Fig. 2, is not different in any significant way from Fig. 1. One immediate corollary is that tip splitting seen in almost isotropic systems must be thought of as *nonlinear* instability, similar to the current ideas regarding tip splitting for Saffman-Taylor fingers. This agrees with the approximate computation of Pelce.[7] More importantly, our results bear directly on the issue of side branching. Our results mean that side branching must be understood via the amplification of *finite* noise as the disturbance moves away from the tip.[13,14] One encouraging fact pointing in this direction is that the most unstable part of our spectrum (and hence most likely to be excited by finite noise) is indeed stationary in the laboratory frame. An approach to the determination of the side-branch wavelength based on this idea will be

presented elsewhere.

The work of one of us (D.K.) was supported by U.S. Department of Energy Grant No. DE-FG-02-85ER54189.

[1]For a recent review, see D. Kessler, J. Koplik, and H. Levine, in Proceedings of NATO Advanced Study Workshop on Pattern Defects and Microstructures, Austin, Texas, March 1986 (to be published).

[2]D. Kessler and H. Levine, Phys. Rev. B **33**, 7687 (1986); D. Kessler, J. Koplik, and H. Levine, Phys. Rev. A **33**, 3352 (1986); D. Meiron, Phys. Rev. A **33**, 2704 (1986).

[3]A. Barbieri, D. Hong, and J. Langer, to be published; M. Ben-Amar and Y. Pomeau, to be published.

[4]P. G. Saffman and G. J. Taylor, Proc. Roy. Soc. London, Ser. A **245**, 312 (1952).

[5]For a discussion of different solidification patterns, see J. S. Langer, Rev. Mod. Phys. **52**, 1 (1980).

[6]J. S. Langer and H. Müller-Krumbhaar, Acta Metall. **26**, 1681, 1689, 1697 (1978); H. Müller-Krumbhaar and J. S. Langer, Acta Metall. **29**, 145 (1981); J. P. Van der Eerden and H. Müller-Krumbhaar, Acta Metall. **34**, 839 (1986).

[7]P. Pelce, thesis, Université de Provence, 1986 (unpublished).

[8]Y. B. Zeldovich, A. G. Isratov, N. Kidin, and V. P. Librovitch, Combust. Sci. Technol. **24**, 1 (1980).

[9]D. Kessler and H. Levine, Discrete Set Selection of Saffman-Taylor Fingers (to be published).

[10]J. M. Vanden-Broeck, Phys. Fluids **26**, 2033 (1983).

[11]B. T. Smith *et al., Matrix Eigensystem Routines—EISPACK Guide,* Lecture Notes in Computer Science Vol. 6, edited by G. Goos and J. Hartmanis (Springer, New York, 1974).

[12]D. Kessler and H. Levine, Phys. Rev. A **33**, 2621,2634 (1986).

[13]R. Deissler, J. Stat. Phys. **40**, 371 (1985).

[14]R. Pieters and J. S. Langer, Phys. Rev. Lett. **56**, 1948 (1986). This paper deals with the boundary-layer model and predicts a side-branching response to even infinitesimal noise. This cannot be true in the full nonlocal system at any nonzero Peclet number.